

Neuroplasticity in F16 fighter jet pilots

by

Eline Radstake

Supervised by:

1. dr. Angelique Van Ombergen
2. Steven Jillings
3. Prof. dr. David Norris

Radboud University Nijmegen

## Table of contents

Abbreviations .....	3
Figures .....	4
Tables .....	4
Abstract .....	5
1. Introduction .....	6
2. Methods .....	8
2.1 Subjects.....	8
2.2 Procedure .....	8
2.3 Data acquisition .....	9
2.4 Data analysis.....	9
2.4.1 Voxel-based morphometry (VBM).....	9
2.4.2 Tract-based spatial statistics (TBSS) .....	10
2.4.3 Intrinsic connectivity contrast (ICC) .....	11
2.4.4 Seed-based analysis .....	11
2.4.5 fMRI task paradigms.....	12
3. Results .....	14
3.1 Voxel-based morphometry (VBM). .....	14
3.2 Tract-based spatial statistics (TBSS).....	14
3.3 Resting state functional connectivity.....	14
3.3.1 ICC .....	14
3.3.2 Seed based analysis.....	15
3.4 Task-based fMRI .....	17
4. Discussion .....	19
4.1 Semantic processing .....	19
4.2 Increase in functional connectivity between vestibular and visual brain area.....	20
4.3 Motor imagery .....	21
4.4 Fighter pilots vs. cosmonauts .....	22
4.5 Replication study .....	22
4.6 Limitations.....	23
5. Conclusion.....	25
Literature .....	26

## Abbreviations

BOLD – blood-oxygen-level dependent	MNI – Montreal Neurological Institute
CSF – cerebrospinal fluid	MRI – magnetic resonance imaging
DLPFC – dorsolateral prefrontal cortex	MTG – middle temporal gyrus
DMFC – dorsomedial frontal cortex	PPC – posterior parietal cortex
FA – fractional anisotropy	rAG – right angular gyrus
fMRI – functional magnetic resonance imaging	RD – radial diffusivity
FSL - FMRIB's software library	ROI – region of interest
FWE – family-wise error	rOP2 – right parietal operculum 2
FWHM – full-width half maximum	rTPJ – right temporo-parietal junction
GLM – general linear model	SCC – semicircular canal
GM – gray matter	SD – standard deviation
HRF – hemodynamic response function	SPL – superior parietal lobule
ICC – intrinsic connectivity contrast	SPM – Statistical Parametric Mapping
IFG – inferior frontal gyrus	TBSS – tract-based spatial statistics
IPL – inferior parietal lobule	TFCE – threshold-free cluster enhancement
lpMTG – left posterior middle temporal gyrus	VBM – voxel-based morphometry
MCC – middle cingulate cortex	VID – visual induced dizziness
MD – mean diffusivity	VN – vestibular nuclei
MI – motor imagery	WM – white matter

## Figures

**Fig 1.** Hypothesis-free investigation of resting state connectivity shows decreased ICC in the left posterior middle temporal gyrus thus this region has a reduced overall connectivity with the rest of the brain in the fighter pilots. Figure shows the statistical map, thresholded at cluster-level family wise error rate  $p < 0.05$  and scaled by t-value. Peak voxel at MNI coordinates  $x = -62$   $y = -36$   $z = -10$ ,  $p = 0.027$  FWE cluster-level (permutation tests), cluster size = 166 voxels. Bars indicate cluster-level effects sizes and error bars at 90% confidence interval..... 15

**Fig 2.** Results of ROI-analysis of the left posterior middle temporal gyrus. Regions of which time series correlated with the time series of the seed region, are shown in yellow/red, negative correlation is shown in blue. Legend represents t-values. Statistical maps have been thresholded at cluster-level family wise error rate  $p < 0.05$ ..... 16

**Fig 3.** Seed in right parietal operculum 2 (rOP2) (top left) shows significant differences between pilots and controls in functional connectivity with left extrastriate cortex. Red regions indicate increased functional connectivity between rOP2 and left extrastriate cortex in the fighter pilots. Legend represents t-values. Statistical maps are thresholded at cluster-level family wise error rate  $p < 0.05$ . Peak voxel at MNI coordinates  $x = -40$   $y = -88$   $z = -18$ ,  $p = 0.032$  FWE cluster level, cluster size = 233 voxels. .... 17

**Fig 4.** Differences in brain activity during fMRI tennis imagery paradigm. Figure shows axial, coronal, and sagittal slices with significant increased brain activity during fMRI tennis imagery paradigm in the fighter pilots as compared to controls. Statistical maps are thresholded at cluster-level family wise error rate  $p < 0.05$  and scaled by  $\log(p)$  with  $\log(p) = 1.3$  equals to  $p = 0.05$ . .... 18

## Tables

**Table 1.** MNI coordinates and sphere radius (r) in mm of spherical ROIs for radial diffusivity analysis. .... 11

**Table 2.** Overview of MNI coordinates and radius (r) in mm of spherical seeds for analysis of resting-state fMRI data. .... 12

**Table 3** Results of ROI analysis of radial diffusivity, showing p-values at specific ROI for each contrast. .... 14

**Table 4.** Results of task-based fMRI tennis imagery paradigm. Table shows regions that have a significant increase in brain activity during tennis imagery versus rest, in fighter pilots as compared to controls. Peak voxels' MNI coordinates are given, as well as cluster size and p-values FWE-corrected at cluster level and uncorrected. .... 17

## Abstract

Fighter jet pilots are exposed to numerous gravitational transitions, which have been shown to influence peripheral vestibular processing. This study investigated the effects of training and g-level transitions on neuroplasticity in fighter jet pilots. We compared 10 male fighter pilots with age-, gender-, and education-matched controls by means of a multimodal MRI protocol. Volumetric and morphometric gray matter, white matter, and cerebrospinal fluid measurements derived from T1 weighted images were evaluated. Whole-brain and region of interest based analysis of WM microstructure was performed using diffusion weighted imaging data. A hypothesis-free and a seed-based approach was used for analysis of resting-state functional connectivity, and finally, group differences in BOLD signal during a tennis and navigation imagery paradigm were analyzed from task-based functional MRI data. Statistical analyses included non-parametric permutation testing, threshold-free cluster enhancement, and a cluster-level familywise error rate to correct for multiple comparisons. We did not find significant group differences in tissue volume and WM microstructure. Hypothesis-free analysis of resting-state fMRI data showed a decreased connectivity between the left posterior middle temporal gyrus and the rest of the brain. Additionally, an increased functional connectivity was found between the seed in the right parietal operculum 2 and the left occipital lobe. During tennis imagery, fighter pilots showed a significant increase in activity in bilateral precuneus, left temporal pole, left inferior parietal lobule, left middle temporal gyrus, and right middle cingulate cortex. The finding of increased functional connectivity between vestibular- and visual brain areas suggests that increased exposure to conflicting sensory information, as experienced during flight, alters brain functional connectivity in a way such that both sensory modalities can better cooperate to solve conflicts in sensory information.

## 1. Introduction

Due to acceleration during aerobatic maneuvers, fighter pilots are exposed to numerous gravitational transitions during flight (Balldin, 2003). The effects of different gravitational environments on neuroplasticity remain unclear. Neuroplasticity is the capacity of the brain to change its structure and function in response to events, and is crucial for skill learning and adaptation to new environments and bodily states (Pearson-Fuhrhop & Cramer, 2010). Differences in brain structure and function between individuals can be explained by differences in experience and learning (Kelly & Castellanos, 2014; Maguire et al., 2000; Scholz, Klein, Behrens, & Johansen-Berg, 2009). Because of the exposure to g-level transitions, fighter pilots are a suitable group to look for the effects of gravitational transitions on neuroplasticity.

During the in-flight aerobatic maneuvers, an intravestibular conflict arises (Tribukait & Eiken, 2012). On Earth, head movements are registered by both the otolith organs, detecting linear translations and head tilt with respect to the gravity vector, and three semicircular canals (SCCs), detecting the angular acceleration (Hain & Helminski, 2014). During maneuvers like coordinated turns, the sum of gravity force and centrifugal force is directed along the body's z-axis (head-to-foot) (Balldin, 2003). As a result, the otolith organs do not sense a tilt. In contrast, the SCCs do sense a tilt in the roll plane. Thus, a conflict arises between the otolith organs and the SCCs (Tribukait & Eiken, 2012).

Studies have shown that fighter pilots have a different sensitivity to these angular displacements as compared to normal controls (Tribukait & Eiken, 2012; Tribukait, Grönkvist, & Eiken, 2011). In both the pitch and roll plane, fighter pilots are more sensitive to information coming from the SCCs. Thus, information coming from the SCCs seems more dominant over information coming from the otolith organs. This is different to normal subjects in which signals coming from the otolith organs are thought to dominate those coming from the SCCs during centrifugation (Tribukait & Eiken, 2005, 2006). This suggests that, as a result of the intravestibular conflict that arises during flight, the brain alters the weighting of information coming from the different parts of the vestibular system in such a way that it is more sensitive to detect changes in angular position (Tribukait & Eiken, 2012).

Furthermore, neuroplasticity due to gravitational transitions has also been observed after parabolic flight. During such a flight, different g-levels are induced ranging from zero g to 1,8 g (Karmali & Shelhamer, 2008). First time exposure to gravitational transitions can also induce changes in brain function. A decrease in intrinsic connectivity contrast (ICC) was found in the right temporo-parietal junction (rTPJ)/angular gyrus (rAG) (Van Ombergen, Wuyts, et al., 2017), a region thought to be involved in the integration of multisensory information for spatial

functioning, such as the perception of verticality (Block, Bastian, & Celnik, 2013; Fiori, Candidi, Acciarino, David, & Aglioti, 2015). During parabolic flight, sensory information coming from visual, proprioceptive and vestibular organs is continuously in conflict, resulting in the inability to determine what is up and down. These results suggest that after exposure to different g-levels, the rTPJ/rAG has reduced participation in whole-brain connectivity (Van Ombergen, Wuyts, et al., 2017).

In line with the effects of transitions in gravitational level on neuroplasticity, several studies have investigated the effects of microgravity on neuroplasticity (Koppelmans, Bloomberg, Mulavara, & Seidler, 2016; Ombergen et al., 2016; D. R. Roberts et al., 2017; Van Ombergen, 2017). Due to the absence of gravitational force acting upon the otolith organs during space flight, the otolith organs no longer detect head orientation with respect to the body's vertical axis, but it remains sensitive to linear translations. However, cosmonauts already show structural differences compared with a healthy control group before spaceflight (Van Ombergen, 2017). This suggests that these groups are not ideally matched, thus it would be beneficial to include a control group that shows more similarities. The pre-existing differences in brain structure are likely due to the extensive training of cosmonauts before spaceflight. Therefore, we expect that fighter jet pilots are a more suitable control group since they have similar training as cosmonauts.

This study aims to investigate the effects of training and g-level transitions on brain structure and function, in fighter jet pilots. By means of a multimodal MRI protocol, we investigated whether there are differences in brain structure and function between F16 fighter pilots and matched controls. Hereto, we evaluated volumetric and morphometric GM, WM, and CSF measurements, WM microstructure, and functional connectivity in both groups. As a result of the alterations of peripheral vestibular signaling in fighter pilots (Tribukait & Eiken, 2012; Tribukait et al., 2011), we expected to see differences in structural and functional MRI measures in F16 fighter pilots compared to controls in vestibular cortical areas. Furthermore, we expected to see similarities in brain plasticity between cosmonauts before spaceflight and fighter pilots.

## 2. Methods

### 2.1 Subjects

Fighter jet pilots were recruited via the Belgian Royal Air Force. Inclusion criteria were: age between 18 and 65, and male. Exclusion criteria were: neurological disease, medication with effects on the CNS, excessive alcohol- and/or drug use, orthopedic disease, vestibular problems, jetlag (at least one week after transcontinental flight/mission) and at least 24 hours since last exposure to high g-levels. A total of 10 fighter pilots were scanned (mean age (SD)=29 (3,2) years; range 23-32 years). A control group (mean age (SD) = 29 (3,2) years; range 23-32 years) of 10 adults was included, matched for age, gender and educational level. Additionally, controls were also matched for handedness (9 right- and 1 left handed in each group). All participants signed an informed consent form. The study was approved by the local ethics committee of the Antwerp University Hospital (13/38/357).

### 2.2 Procedure

Prior to the scan session, participants completed the Edinburgh Handedness Inventory (<http://www.brainmapping.org/shared/Edinburgh.php>) (Oldfield, 1971). A laterality index is calculated, where a score of 100 reflects complete right-handedness and a score of -100 reflects complete left-handedness. Additionally, participants completed a MRI safety screenings form.

We used a 32-channel head coil for the T1- and T2- weighted images, the diffusion weighted images, and a resting-state sequence. For the resting-state acquisition, subjects were told to lay with their eyes closed, not to sleep, and not to think about anything in particular. Instructions were given prior to the experiment and at the start of the sequence.

After the resting-state sequence, two task fMRI sequences were acquired. Instructions for the tasks were given through a headphone, which necessitated us to use a 20-channel head coil to fit in the headphones. Additionally, a T1 weighted image was acquired with the 20-channel head coil for anatomical registration of the functional images. During the first task fMRI session, subjects were asked to imagine playing tennis. In the second session, subjects were asked to imagine navigating through their house. During each session, blocks of task were alternated with blocks of rest with equal duration. Each session started and ended with a rest block. In total, there were 6 blocks of the rest condition and 5 blocks of the task condition. Subjects were told to close their eyes during both fMRI sessions.

## 2.3 Data acquisition

All data were acquired on a 3T Siemens MAGNETOM PrismaFit scanner (Siemens, Erlangen, Germany). A 32-channel head coil was used for the anatomical images, diffusion-weighted images and the resting state data, while a 20-channel head coil was used for the task fMRI data acquisition as well as a second T1 weighted image for fMRI co-registration purposes.

The T1-weighted anatomical images were acquired using a MPRAGE sequence (TR=2000ms; TE=3.05ms; flip angle=8°; voxel size=1.0 x 1.0 x 1.0 mm). Additionally, a T2-weighted anatomical image was acquired with a 32-channel head coil, using a SPACE sequence (TR=3200ms; TE=408ms; voxel size=0.9 x 0.9 x 0.9 mm).

Two sets of whole brain diffusion weighted volumes, acquired in opposite phase encoding directions, were obtained using single shot echo-planar imaging (EPI) sequence with the following parameters: MB factor=2; GRAPPA factor=2; voxel size=2.0x2.0x2.0; matrix=120x120; 68 slices; TR=3560ms; TE=72,60ms. Volumes were acquired for 25 directions at  $b=700\text{smm}^{-2}$ ; 45 directions at  $b=1200\text{smm}^{-2}$ ; 75 directions at  $b=2800\text{smm}^{-2}$ ; flip angle=90°. In addition, 6 volumes without diffusion weighting ( $b=0\text{smm}^{-2}$ ) were acquired.

During resting state, whole brain T2\*-weighted images were acquired using a gradient-echo EPI sequence (TR=748ms; TE=31ms; volumes=350 flip angle=70°; voxel size=2x2x2mm; field of view=212x212mm; matrix size=106x106x72).

For task fMRI data, whole brain T2\*-weighted images were acquired using a gradient-echo EPI sequence (TR=2540ms; TE=30ms; volumes=65 flip angle=77°; voxel size=3x3x3mm; field of view=192x192mm; matrix size=64x64x42). For all functional MRI sequences, acquisition started with 4 dummy scans, which were immediately discarded to account for T1 saturation effects.

## 2.4 Data analysis

### 2.4.1 Voxel-based morphometry (VBM)

Data preprocessing and analysis was performed with the CAT12 Toolbox by Christian Gaser & Robert Dahnke (Department of Psychiatry, University of Jena, Jena, Germany; <http://www.neuro.uni-jena.de/cat/>) using Statistical Parametric Mapping 12 (SPM12 v7219; <http://www.fil.ion.ucl.ac.uk/spm/>) implemented in MATLAB R2017b (The Mathworks Inc., Natick, MA, USA). Preprocessing steps included spatial normalization into the Montreal Neurological Institute (MNI) space using DARTEL normalization (Ashburner, 2007), segmentation and modulation (non-linear only) to adjust for volume changes during

normalization, and smoothing with a Gaussian kernel of 8mm full width at half maximum (FWHM). Additionally, the quality control function of the CAT12 Toolbox was used to assess sample homogeneity of the preprocessed data. To test for volume differences in GM, WM, and CSF between groups, a two-sample t-test was used. We applied threshold-free cluster enhancement (TFCE) (Stephen M. Smith & Nichols, 2009) (SPM's TFCE toolbox developed by Christian Gaser; <http://dbm.neuro.uni-jena.de/tfce/>) and permutation test with 5000 permutations to obtain voxel-level p-values. These were corrected for multiple comparisons with FWER  $p < 0.05$ . Age and flight hours in a F16 jet were implemented as covariates in the statistical model.

#### **2.4.2 Tract-based spatial statistics (TBSS)**

For the analysis of the DTI data, we replicated the study of Roberts and colleagues (R. E. Roberts, Anderson, & Husain, 2010). Preprocessing steps included denoising, gibbs-ringing artefact correction, motion and distortion correction, and bias field correction. These steps were performed using MRtrix3 (<http://www.mrtrix.org/>). Voxel-wise statistical analysis of the fractional anisotropy (FA) data was carried out using tract-based spatial statistic (TBSS) (S M Smith et al., 2006), part of the FMRIB's software library (FSL) (Stephen M. Smith et al., 2004). TBSS projects all subjects' FA data onto a mean FA skeleton, before applying voxel-wise cross-subject statistics. The same procedure was carried out for the mean diffusivity (MD) images. A between group voxel-wise comparison analysis included permutation-based non-parametric testing, with a FWE correction for multiple comparison at  $p < 0.05$ .

For the replication of the ROI analysis, spherical ROIs were generated using the center coordinates from the ROIs of Roberts and colleagues (R. E. Roberts et al., 2010). Then, white matter ROIs were generated using the overlap between the spherical ROIs and the white matter skeleton. This resulted in eight bilateral ROIs in the dorsomedial frontal cortex (DMFC), posterior parietal cortex (PPC), inferior frontal gyrus (IFG), and dorsolateral prefrontal cortex (DLPFC). For an overview of the MNI coordinates and sphere radius, readers are referred to Table 1. A voxel-wise comparison analysis between the groups of radial diffusivity (RD) in each ROI was performed, using permutation-based non-parametric testing, and FWE correction for multiple comparison at  $p < 0.05$ .

**Table 1.** MNI coordinates and sphere radius (r) in mm of spherical ROIs for radial diffusivity analysis.

	left hemisphere			right hemisphere			r (mm)
	x	y	z	x	y	z	
Inferior frontal gyrus	-40	26	16	43	27	13	7
Dorsolateral prefrontal cortex	-35	24	30	36	26	28	5
Pre-supplementary motor area	-14	19	53	14	19	52	7
Posterior parietal cortex	-44	-53	34	43	-54	36	10

### 2.4.3 Intrinsic connectivity contrast (ICC)

Statistical Parametric Mapping 12 (SPM12; <http://www.fil.ion.ucl.ac.uk/spm/>) implemented in MATLAB R2017b (The Mathworks Inc., Natick, MA, USA) was used for preprocessing. Steps included slice timing correction, realignment, co-registration of functional to structural space, segmentation of structural data, normalization into standard stereotactic Montreal Neurological Institute (MNI) space, and spatial smoothing using a Gaussian kernel of 8 mm FWHM.

For the resting state statistical analysis, the CONN v.17 functional connectivity toolbox ([www.nitrc.org/projects/conn](http://www.nitrc.org/projects/conn)) was used. Additional to the preprocessing steps, denoising was done by applying linear regression and band-pass filtering to remove motion, physiological, and other artifacts from the BOLD signal. Six outlier scans in the control- and 4 in the pilot group related to motion were detected and removed from the data. For the anatomical component-based noise correction (aCompCor), significant principal components are derived from WM and CSF. These components are included as nuisance parameters in the first-level general linear model (GLM) (Behzadi, Restom, Liau, & Liu, 2007). Additionally, 12 parameters (3 translations, 3 rotations and their derivatives) of head motion were also added as regressors to the GLM. A temporal band-pass filter of 0.008-0.09Hz was applied.

For each subject, Intrinsic Connectivity Contrast (ICC) was computed for each voxel in the brain. This is a hypothesis-free method to measure the strength of the connectivity between one voxel and the rest of the brain (Martuzzi et al., 2011). For the second-level group analysis, a permutation based non-parametric statistical test with 1000 permutations was carried out ( $p < 0.001$  uncorrected and  $p < 0.05$  FWE-corrected at cluster level).

### 2.4.4 Seed-based analysis

An ROI connectivity analysis was performed on the region that showed significant decrease in ICC in the fighter pilots. This was done to identify altered connections of the network associated with the identified node (Martuzzi et al., 2011). Time series of the seed

voxels were averaged together and this was used to estimate whole-brain correlation measures in the fighter pilots. Non-parametric permutation tests were used together with FWE  $p < 0.05$  correction for multiple comparisons.

Besides a hypothesis-free method, we also used seed regions to analyze the resting-state functional data. Seed regions were chosen that were previously proven to be affected by gravitational transitions in naïve subjects, namely the right temporal-parietal junction (rTPJ) (10 mm sphere around MNI coordinates 58 -64 18) (Van Ombergen, Wuyts, et al., 2017), and the superior parietal lobule (SPL) which shows reduced GM volume in cosmonauts preflight (selected based on FSL Harvard Oxford Atlas) (Van Ombergen, 2017). Furthermore, we chose seed-regions that have been shown to be involved in vestibular and visual processing and integration. We used the same seed-regions as the study by van Ombergen (2017) et al. For an overview of these regions readers are referred to Table 2 (Van Ombergen, Heine, et al., 2017). Correlation measures were calculated between the seed BOLD time series and each voxel's BOLD time series. For bilateral seeds, time series of both hemispheres were averaged together. Second-level analysis included permutation-based non-parametric testing for group differences and FWE correction for multiple comparison at  $p < 0.05$  at cluster level.

**Table 2.** Overview of MNI coordinates and radius (r) in mm of spherical seeds for analysis of resting-state fMRI data.

	left hemisphere			right hemisphere			r (mm)
	x	y	z	x	y	z	
<b><u>Visual system</u></b>							
Associative visual cortex	-30	-89	20	30	-89	20	10
Secondary visual cortex	-6	-78	10	6	-78	10	10
Primary visual cortex	-8	-85	10	13	-85	10	6
<b><u>Vestibular processing network</u></b>							
rOP2				42	-24	18	5
Precuneus	0	-52	27				10
Inferior parietal lobule	-51	-51	36	51	-47	42	10
Vestibular nuclei	-16	-36	-32	16	-36	32	5
Thalamus	0	-12	9				4

rOP2: right parietal operculum 2

#### 2.4.5 fMRI task paradigms

For the statistical analysis of the task fMRI data, SPM12 implemented in MATLAB R2017b was used. For each subject, the preprocessed fMRI time series were analyzed using a

blocked design and the GLM. For each task, the time series of the conditions and resting period were modeled. The hemodynamic responses were modeled by convolving a canonical hemodynamic response function (HRF) with a box function. Denoising of the BOLD signal was done by adding 6 motion parameters as regressors to the GLM. A high-pass filter with cut-off of 128 seconds was applied to the data. To identify the brain regions corresponding to each condition, the time series during rest were subtracted from the time series during the task condition. For the second-level analysis we applied TFCE (Smith & Nichols, 2009) (SPM's TFCE toolbox developed by Dr. Gaser) and a permutation test with 5000 permutations to obtain voxel-level p-values. These were corrected for multiple comparisons with FWE  $p < 0.05$ . Results were visualized using MRICroGL by Chris Rorden ([https://www.nitrc.org/frs/?group\\_id=889](https://www.nitrc.org/frs/?group_id=889)) as overlays onto the mean images derived from the entire cohort.

### 3. Results

#### 3.1 Voxel-based morphometry (VBM).

VBM analysis revealed no significant group differences in GM, WM, and CSF tissue volume. Furthermore, ROI analysis of group differences in GM volume of the SPL also showed no significant differences.

#### 3.2 Tract-based spatial statistics (TBSS)

The TBSS analysis did not show any significant group differences in whole brain FA and MD measures. Additionally, there were no significant group differences in the ROI analysis of RD. A borderline significant decrease in RD was found in the left PPC in fighter pilots, compared to controls. This almost reached statistical significance with  $p=0.06$  (peak voxel:  $x,y,z=[-35, -56, 31]$ ). We could not replicate the findings from Roberts and colleagues (2010) (see Table 3 for an overview of peak p-values of all the ROIs).

**Table 3** Results of ROI analysis of radial diffusivity, showing p-values at specific ROI for each contrast.

	<b>Controls &gt; Pilots</b>	<b>Pilots &gt; Controls</b>
IFG left	0.452	0.731
IFG right	0.480	0.386
DLPFC left	0.313	0.503
DLPFC right	0.782	0.721
PreSMA left	0.113	0.252
PreSMA right	0.230	0.176
PPC left	0.060	0.543
PPC right	0.311	0.218

IFG: inferior frontal gyrus; DLPFC: dorsolateral prefrontal cortex; PreSMA: pre-supplementary motor area; PPC: posterior parietal cortex

#### 3.3 Resting state functional connectivity

##### 3.3.1 ICC

We compared intrinsic functional connectivity between fighter pilots and controls. The results of the intrinsic connectivity contrast analysis showed a decrease in intrinsic connectivity in the left middle temporal gyrus in the fighter pilots (Figure 1).

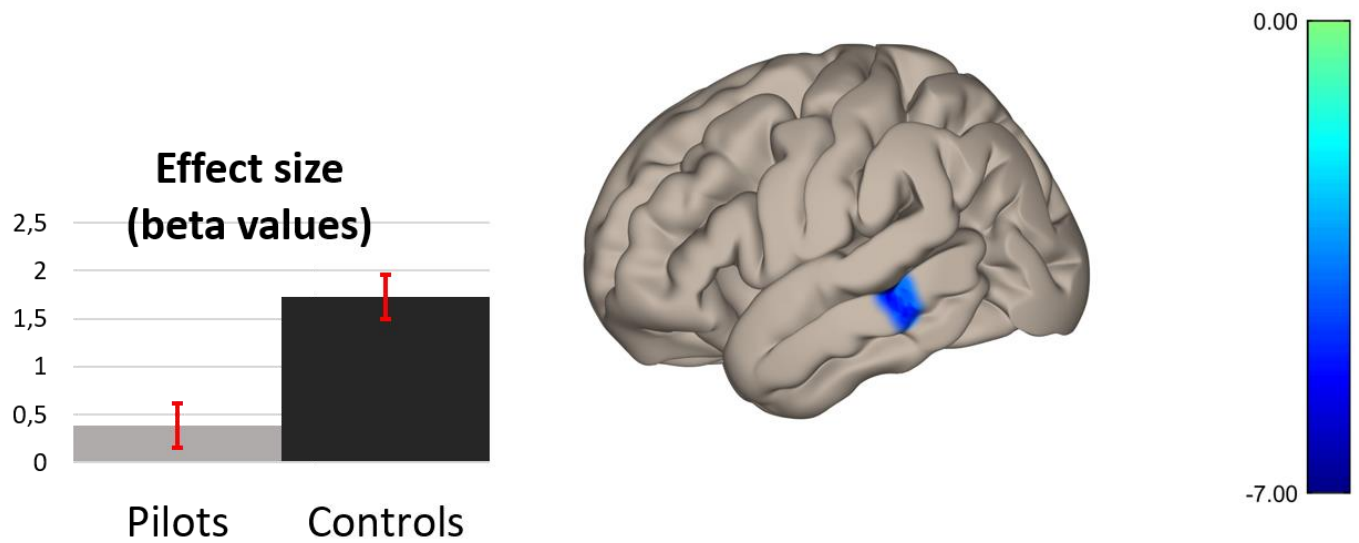


**Fig 1.** Hypothesis-free investigation of resting state connectivity shows decreased ICC in the left posterior middle temporal gyrus. Figure shows the statistical map, thresholded at cluster-level family wise error rate  $p < 0.05$  and scaled by t-value. Peak voxel at MNI coordinates  $x = -62$   $y = -36$   $z = -10$ ,  $p = 0.027$  FWE cluster-level (permutation tests), cluster size = 166 voxels. Bars indicate cluster-level effects sizes and error bars at 90% confidence interval.

### 3.3.2 Seed based analysis.

The left MTG was then used as a seed area to perform ROI analysis in the fighter pilot group in order to better comprehend the network associated with this region. Areas, of which time series correlated with that of the ROI, were located in bilateral superior/middle/inferior temporal gyri, inferior/middle/superior frontal gyri, angular gyri, lateral occipital cortexes and posterior cingulate gyrus/precuneus. Areas with negative correlating time series were found in bilateral supramarginal gyri, parietal opercula, insular cortexes, superior frontal gyri, and anterior cingulate gyrus (Figure 2).

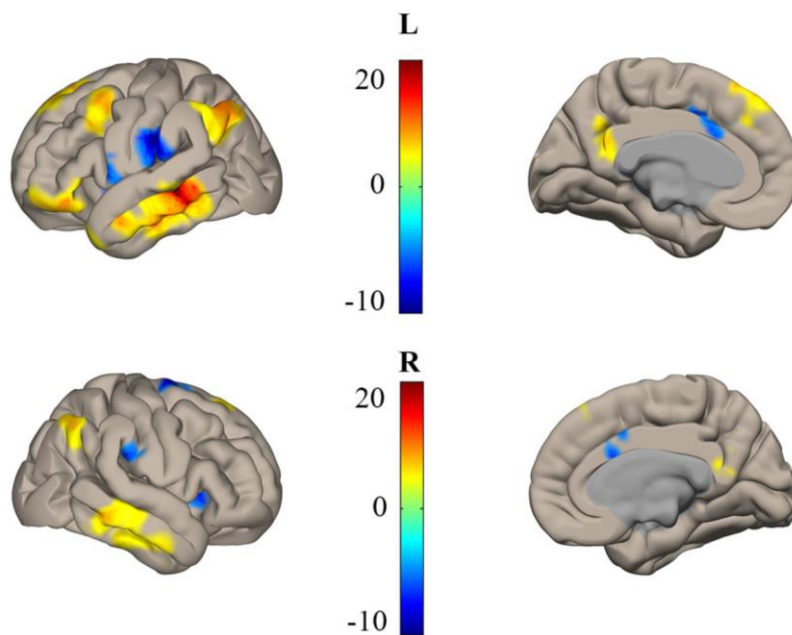


**Fig 2.** Results of ROI-analysis of the left posterior middle temporal gyrus. Regions of which time series correlated with the time series of the seed region, are shown in yellow/red, negative correlation is shown in blue. Legend represents t-values. Statistical maps have been thresholded at cluster-level family wise error rate  $p < 0.05$ .

We found a significant increase in functional connectivity between the rOP2 and left middle and inferior occipital gyri in the fighter pilots compared to controls (Figure 3). For the other seeds, we did not find any significant group differences in functional connectivity.

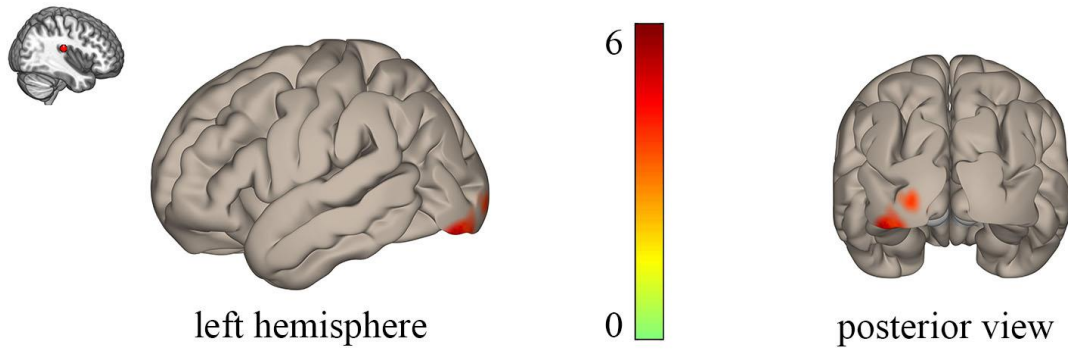


**Fig 3.** Seed in right parietal operculum 2 (rOP2) (top left) shows significant differences between pilots and controls in functional connectivity with left extrastriate cortex. Red regions indicate increased functional connectivity between rOP2 and left extrastriate cortex in the fighter pilots. Legend represents t-values. Statistical maps are thresholded at cluster-level family wise error rate  $p < 0.05$ . Peak voxel at MNI coordinates  $x = -40$   $y = -88$   $z = -18$ ,  $p = 0.032$  FWE cluster level, cluster size = 233 voxels.

### 3.4 Task-based fMRI

We looked for group differences in BOLD signal changes during mental imagery paradigms. No significant group differences were found during the navigation paradigm. However, for the tennis paradigm, the results showed an increase in activity in the fighter pilot group in the bilateral precuneus, left temporal pole, left inferior parietal lobule (IPL), left middle temporal gyrus (MTG), right midcingulate cortex (MCC) during tennis (Table 4; Figure 4).

**Table 4.** Results of task-based fMRI tennis imagery paradigm. Table shows regions that have a significant increase in brain activity during tennis imagery versus rest, in fighter pilots as compared to controls. Peak voxels' MNI coordinates are given, as well as cluster size and p-values FWE-corrected at cluster level and uncorrected.

	Peak			Cluster size	Cluster p -value FWE corrected	P uncorrected peak
	X	Y	Z			
Precuneus	2	-65	64	542	0.030	0.008
Left temporal pole	-52	14	-8	88	0.039	0.010
Left IPL	-46	-44	60	27	0.040	0.002
Left MTG	-38	-60	20	33	0.041	0.009
Right MCC	2	4	42	138	0.044	0.013

IPL: inferior parietal lobule; MTG: middle temporal gyrus; MCC: middle cingulate cortex.

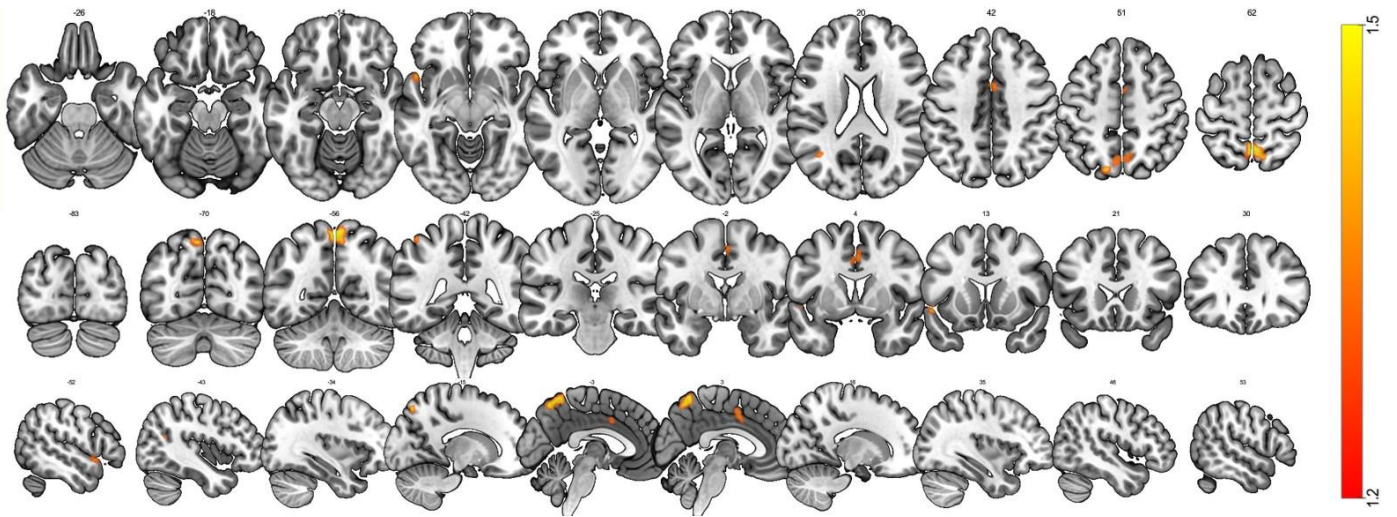


**Fig 4.** Differences in brain activity during fMRI tennis imagery paradigm. Figure shows axial, coronal, and sagittal slices with significant increased brain activity during fMRI tennis imagery paradigm in the fighter pilots as compared to controls. Statistical maps are thresholded at cluster-level family wise error rate  $p < 0.05$  and scaled by  $\log(p)$  with  $\log(p) = 1.3$  equals to  $p = 0.05$ .

## 4. Discussion

This study investigated possible differences in brain structure and function between fighter jet pilots and matched controls by means of multimodal MRI analyses. Structural measures include volumetric and morphometric GM, WM, and CSF measurements, as well as diffusion metrics derived from diffusion weighted imaging (DWI). We did not find any significant group differences in brain tissue volume or white matter microstructure. For the functional analysis, both resting-state and task-based fMRI data were collected. With a hypothesis-free approach, we found a decrease in intrinsic connectivity contrast (ICC) in the left posterior middle temporal gyrus in the fighter pilots, when compared with controls. Further ROI analysis of the lpMTG showed increase in functional connectivity during rest in frontal-, temporal-, and parietal brain regions. Additionally, the seed-based analysis showed an increase in functional connectivity between the rOP2 and extrastriate regions in the left occipital cortex. For the task-based fMRI data we did not find any significant group differences in navigation imagery paradigm. For tennis imagery, we found increased activity in the fighter pilot group in the bilateral precuneus, left temporal pole, left inferior parietal lobule (IPL), left middle temporal gyrus (MTG), right midcingulate cortex (MCC) during tennis.

### 4.1 Semantic processing

We find a decreased ICC in the left posterior middle temporal gyrus (lpMTG) in the fighter pilots. This suggests that the lpMTG has a reduced overall connectivity with the rest of the brain in the fighter pilots. To better comprehend the network associated with the lpMTG, we additionally performed a ROI analysis on the resting-state data of the fighter pilots (Martuzzi et al., 2011). A network of brain areas that were positively correlated with the lpMTG was identified.

Previous studies suggest that the lpMTG is involved in processing of language. More specifically, in case of high semantic ambiguity, that is when one word has multiple meanings, there is an increase in brain activity in this network (Rodd, Davis, & Johnsrude, 2005; Tesink, Petersson, Berkum, Buitelaar, & Hagoort, 2014; Zempleni, Renken, Hoeks, Hoogduin, & Stowe, 2007). Also, the network identified by our seed-based analysis shows an overlap with previously indicated resting-state network of language processing (Muller & Meyer, 2014). Fighter pilots use a specific code language in which everyday words have a different meaning, thus with a lot of semantic ambiguous words. This use of code language might be a possible explanation for the altered connectivity we see in the lpMTG. However,

with the present data, this only remains a speculation. Future, more hypothesis-driven studies could aim on investigating how the use of a code language can influence brain activity.

#### **4.2 Increase in functional connectivity between vestibular and visual brain area.**

An aim of this study was to investigate whether the alterations in peripheral vestibular signaling in the fighter pilots (Tribukait & Eiken, 2012; Tribukait et al., 2011) could be detected at the level of the brain through neuroimaging analysis. Seed based analysis showed an increase in functional connectivity between the right parietal operculum 2 (rOP2) and the left extrastriate cortex. The rOP2 was chosen as a seed area since previous studies have suggested this area is a key vestibular cortical area (Zu Eulenburg, Caspers, Roski, & Eickhoff, 2012).

Previous studies have indicated a mechanism, which involves vestibular and visual brain areas. Brandt and colleagues (1998) proposed a reciprocal inhibitory visual-vestibular interaction, which provides a mechanism for shifting the dominant sensorial weight from one modality to the other (Thomas Brandt, Bartenstein, Janek, & Dieterich, 1998; Della-Justina et al., 2014; Lopez & Blanke, 2011; Naito, 2003). Visual stimulation will thus deactivate vestibular cortical regions and vice versa, which has been replicated numerous times in fMRI studies (for a review readers are referred to (Lopez & Blanke, 2011)). Also, during situations of conflicting vestibular and visual input, this mechanism avoids perceptual ambiguity by shifting the sensorial weight to the more reliable modality (T Brandt et al., 2002). An example of such a conflict is the apparent feeling of self-motion during full-field visual motion stimulation, for instance, the sensation of self-movement while watching another train depart from an adjacent track in a train station.

Alterations in connectivity in vestibular and visual brain areas have also been described in a population of patients with visual induced dizziness (VID) (Van Ombergen, Heine, et al., 2017). When exposed to complex or moving visual triggers, VID patients experience symptoms of vestibular dysfunction (Bronstein, 1995). VID patients thus present with an overreliance on visual information. A reduced ICC was found in the right central operculum and an increase in ICC was found in the occipital pole when comparing VID patients to healthy controls. These alterations in the visual and vestibular cortical networks seem to reflect the increased weight of the visual system and are thought to underlie the symptoms of VID patients (Van Ombergen, Heine, et al., 2017).

Fighter pilots experience multiple sensory conflicts during flight. As previously explained, the perceived acceleration parallel to the body's z-axis during a coordinated turn

results in an intravestibular conflict. Furthermore, conflict between vestibular and visual signals also arises during these maneuvers, as visual information registers a body tilt, while the otolith organs do not. The increase in functional connectivity between vestibular and visual regions in the fighter pilots suggests that these regions might cooperate more closely to solve the conflicts in sensory information. To better understand how this mechanism works in fighter pilots, future studies could investigate brain activity of fighter pilots during unimodal or multimodal visual- and vestibular stimulation.

### **4.3 Motor imagery**

For the task-based fMRI data, subjects had to imagine playing tennis. Mental imagery is a task-paradigm that is capable of activating neural components that are correlated with actual execution of the task. During motor imagery (MI), a subject imagines executing a voluntary movement, without actually executing the movement. As a result, unconscious motor preparations that share common neural mechanisms with the conscious executions of that particular movement, are activated (Jeannerod, 1994, 1995). Fighter pilots showed an increase in activity in the bilateral precuneus, the left inferior parietal lobule (IPL), the right middle cingulate cortex (MCC), left temporal pole and left MTG.

Several studies have shown that the involvement of the posterior parietal cortex, including the precuneus, and the IPL are crucial for MI performance (Fleming, Stinear, & Byblow, 2010; Kraeutner, Keeler, & Boe, 2016; Lebon, Horn, Domin, & Lotze, 2018; Schulz, Ischebeck, Wriessnegger, Steyrl, & Müller-Putz, 2018; Sladky et al., 2016; Zhang & Li, 2012). Picard and Strick suggested the existence of cingulate motor regions in the human brain (N Picard & Strick, 1996; Nathalie Picard & Strick, 2001) and this has been supported by a neuroimaging study (Amiez & Petrides, 2014). Previous studies have indicated that different imagining strategies are mediated through separate brain regions (Guillot et al., 2009; Solodkin, Hlustik, Chen, & Small, 2004). Especially during MI which involves spatially complex situations, with shifts of spatial attention between objects or locations, the PPC (including the precuneus) seems to be important (Schulz et al., 2018). Furthermore, the precuneus, left temporal pole, and left MTG have been associated with mentalizing and perspective taking (Cavanna & Trimble, 2006; Den Ouden, Frith, Frith, & Blakemore, 2005; Ruby & Decety, 2004) Our finding of increased activity during MI in these areas in the fighter pilots could possibly be explained by different MI strategies. However, since we did not collect any behavioral data, we can only speculate about the observed differences.

#### **4.4 Fighter pilots vs. cosmonauts**

Another aim of this study was to investigate whether F16 fighter pilots show similarities in neuroplasticity with a cohort of cosmonauts, of which data was acquired by the same research group. Cosmonauts already show differences in GM volume with normal controls before spaceflight, as for instance seen in the left SPL and the right precuneus (Van Ombergen, 2017). These differences could be due to the training of the cosmonauts. Since fighter pilots have a similar training, we expected to see similarities in neuroplasticity between fighter pilots and cosmonauts. However, we did not find any group differences in GM volume between fighter pilots and controls. Therefore, the preflight structural differences that we see in the cosmonaut cohort are probably not due to their training. Most cosmonauts in the study were not first-time flyers, therefore the preflight differences between cosmonauts and controls could reflect a persisting effect of previous spaceflight experience (Van Ombergen, 2017). Furthermore, the functional data of the cosmonauts is possibly more suitable to answer the question if there are similarities in neuroplasticity between fighter pilots and cosmonauts. This is because we only see differences between fighter pilots and controls in the functional data, which are thought to be a result of their training.

Although fighter pilots and cosmonauts have a similar training and are both exposed to g-force transitions, it remains difficult to directly compare the data of both groups. One reason for this is the age difference between the groups. The age of astronauts and cosmonauts during their first mission to the ISS is approximately in the mid-forties (Goel et al., 2014), while the average age of fighter pilots in our study was 29. It is possible that there are already significant differences in WM and GM tissue volume between cosmonauts and fighter pilots, as a result of age difference. Both cross-sectional and longitudinal data show regional changes in GM and WM tissue volume related to age (Bartzokis et al., 2001; Raz et al., 2005). Another reason that makes it difficult to compare data from cosmonauts and fighter pilots is the different MRI scanner, which was used to collect data from each group. Instrument-related differences, such as scanner manufacturer, and differences in hardware components affect the variability in MR measures and should be adjusted for (Han et al., 2006).

#### **4.5 Replication study**

A previous study indicated group differences in radial diffusivity (RD) in parietal and frontal brain regions in fighter pilots by using tract-based spatial statistics (TBSS). The changes in RD in these areas correlated with measures of cognitive performance, indicating a possible mechanism of structural white matter alterations in fighter pilots with respect to their cognitive

performance (R. E. Roberts et al., 2010). We could not replicate the findings from Roberts and colleagues (R. E. Roberts et al., 2010), which raises some questions to whether or not the effects that are found in both studies are reliable.

RD was chosen as a measure of WM microstructure as it is thought to reflect an index of myelination (Song et al., 2005). However, studies that have linked RD with myelination were performed in rodent models which have a simple white matter architecture, in terms of number of fiber populations with different directions in a voxel (De Santis, Drakesmith, Bells, Assaf, & Jones, 2014). Diffusion derived measures are highly dependent on architectural complexity (De Santis et al., 2014). It has been estimated that a large amount (~90%) of voxels have multiple fiber population, which has a large influence on the interpretation of anisotropy, and radial/axial diffusivity measures (Jeurissen, Leemans, Tournier, Jones, & Sijbers, 2013). Given the complexity of the WM architecture in the ROIs chosen for this analysis, high variance of RD in these regions could have an impact on finding significant group differences, and therefore, on our replication study.

In brain regions with complex architecture and multiple fibers within a voxel, multi-compartment models could provide more specific measures of axonal properties (De Santis et al., 2014). Fixel-based analysis (FBA) is a method to estimate parameters of fiber density for individual fiber populations within each voxel, which are called fixels (Raffelt et al., 2017). We also performed FBA to identify group differences in WM microstructure. However, we did not find any significant group differences in FBA. A reason for this could be the relative small sample size of our study. As shown by De Santis and colleagues, more advanced metrics of diffusion MRI require larger sample sizes to obtain sufficient statistical power of 0.9 (De Santis et al., 2014).

#### **4.6 Limitations**

Due to the limited number of fighter pilots available for voluntary participation to our study, the sample size in the present study is relative small, which limits the generalization of the present findings. Therefore, future studies should aim on gathering data from larger sample sizes. Another limitation of the present study is the fact that fighter pilots are a very select group of people. Therefore, finding a matched control group remains difficult and some differences between the fighter pilots and the control group still remain. For instance, we did not match for fitness, which might have confounded some of our results. Future studies that would investigate effects of training could aim to include other control groups as for instance

military personnel without flight training, our recruits that did not receive a specific fighter pilot training.

Furthermore, future studies could use the findings of this study to conduct more hypothesis-driven research. The fact that we only find significant group differences in the functional data indicates that future studies should focus more on investigating differences in functional connectivity and brain function. As for instance the finding of increased functional connectivity between vestibular and visual brain areas, future studies could investigate brain activity of fighter pilots during sensory conflict. This could help to better understand the mechanisms behind the altered weighting of vestibular signals in the fighter pilots.

## **5. Conclusion**

We found decreased intrinsic connectivity strength in the left posterior middle temporal gyrus in the fighter pilots during rest, possibly related to an altered semantic processing. Additionally, fighter pilots showed increased brain activity compared to controls in areas involved in mentalizing and motor planning during tennis imagery. Finally, we found increased functional connectivity between visual- and vestibular brain networks in fighter pilots which might have resulted from multisensory conflicts that fighter pilots experience during flight. To increase our understanding of how the interaction between visual- and vestibular brain regions is altered in the fighter pilots, future studies could aim to investigate the (de)activation of these regions during uni- and multimodal stimulation. Our findings show neuroplasticity in fighter pilots, likely to be caused by their specific training and specific stimuli they are exposed to during flight. A better understanding of the mechanisms behind altered visual- and vestibular brain connectivity could also have clinical implications in for instance rehabilitation of vestibular patients.

## Literature

- Amiez, C., & Petrides, M. (2014). Neuroimaging evidence of the anatomo-functional organization of the human cingulate motor areas. *Cerebral Cortex*, *24*(3), 563–578. <https://doi.org/10.1093/cercor/bhs329>
- Ashburner, J. (2007). A fast diffeomorphic image registration algorithm. *NeuroImage*, *38*(1), 95–113. <https://doi.org/10.1016/j.neuroimage.2007.07.007>
- Balldin, U. L. F. I. (2003). Acceleration effects on fighter pilots. In R. Pandolf KB, Burr (Ed.), *Medical aspects of harsh environments* (Vol. 2, pp. 1014–1027).
- Bartzokis, G., Beckson, M., Lu, P. H., Nuechterlein, K. H., Edwards, N., & Mintz, J. (2001). Age-related changes in frontal and temporal lobe volumes in men: a magnetic resonance imaging study. *Archives of General Psychiatry*, *58*(5), 461. Retrieved from <http://archpsyc.ama-assn.org/cgi/content/abstract/58/5/461>
- Behzadi, Y., Restom, K., Liau, J., & Liu, T. T. (2007). A component based noise correction method (CompCor) for BOLD and perfusion based fMRI. *NeuroImage*, *37*(1), 90–101. <https://doi.org/10.1016/j.neuroimage.2007.04.042>
- Block, H., Bastian, A., & Celnik, P. (2013). Virtual Lesion of Angular Gyrus Disrupts the Relationship between Visuoproprioceptive Weighting and Realignment. *Journal of Cognitive Neuroscience*, *25*(4), 636–648. [https://doi.org/10.1162/jocn\\_a\\_00340](https://doi.org/10.1162/jocn_a_00340)
- Brandt, T., Bartenstein, P., Janek, A., & Dieterich, M. (1998). Reciprocal inhibitory visual-vestibular interaction. Visual motion stimulation deactivates the parieto-insular vestibular cortex. *Brain*, *121*(9), 1749–1758. <https://doi.org/10.1093/brain/121.9.1749>
- Brandt, T., Glasauer, S., Stephan, T., Bense, S., Yousry, T. A., Deutschländer, A., & Dieterich, M. (2002). Visual-vestibular and visuovisual cortical interaction. New insights from fMRI and PET. *New York Academy of Sciences*, *956*, 230–241.
- Bronstein, A. M. (1995). Visual vertigo syndrome: Clinical and posturography findings. *Journal of Neurology, Neurosurgery, and Psychiatry*, *59*, 472–476. Retrieved from <https://academic.oup.com/brain/article-lookup/doi/10.1093/brain/awg165>
- Cavanna, A. E., & Trimble, M. R. (2006). The precuneus: A review of its functional anatomy and behavioural correlates. *Brain*, *129*(3), 564–583. <https://doi.org/10.1093/brain/awl004>
- De Santis, S., Drakesmith, M., Bells, S., Assaf, Y., & Jones, D. K. (2014). Why diffusion tensor MRI does well only some of the time: Variance and covariance of white matter tissue microstructure attributes in the living human brain. *NeuroImage*, *89*, 35–44. <https://doi.org/10.1016/j.neuroimage.2013.12.003>
- Della-Justina, H. M., Gamba, H. R., Lukasova, K., Nucci-da-Silva, M. P., Winkler, A. M., &

- Amaro, E. (2014). Interaction of brain areas of visual and vestibular simultaneous activity with fMRI. *Experimental Brain Research*, 233(1), 237–252.  
<https://doi.org/10.1007/s00221-014-4107-6>
- Den Ouden, H. E. M., Frith, U., Frith, C., & Blakemore, S. J. (2005). Thinking about intentions. *NeuroImage*, 28(4), 787–796.  
<https://doi.org/10.1016/j.neuroimage.2005.05.001>
- Fiori, F., Candidi, M., Acciarino, A., David, N., & Aglioti, S. M. (2015). The right temporoparietal junction plays a causal role in maintaining the internal representation of verticality. *Journal of Neurophysiology*, 114(5), 2983–2990.  
<https://doi.org/10.1152/jn.00289.2015>
- Fleming, M. K., Stinear, C. M., & Byblow, W. D. (2010). Bilateral parietal cortex function during motor imagery. *Experimental Brain Research*, 201(3), 499–508.  
<https://doi.org/10.1007/s00221-009-2062-4>
- Goel, N., Bale, T. L., Epperson, C. N., Kornstein, S. G., Leon, G. R., Palinkas, L. A., ... Dinges, D. F. (2014). Effects of Sex and Gender on Adaptation to Space: Behavioral Health. *Journal of Women's Health*, 23(11), 975–986.  
<https://doi.org/10.1089/jwh.2014.4911>
- Guillot, A., Collet, C., Nguyen, V. A., Malouin, F., Richards, C., & Doyon, J. (2009). Brain activity during visual versus kinesthetic imagery: An fMRI study. *Human Brain Mapping*, 30(7), 2157–2172. <https://doi.org/10.1002/hbm.20658>
- Hain, T. C., & Helminski, J. O. (2014). Anatomy and Physiology of the Normal Vestibular System. In *Vestibular Rehabilitation* (pp. 2–18). F. A. Davis Company.
- Han, X., Jovicich, J., Salat, D., van der Kouwe, A., Quinn, B., Czanner, S., ... Fischl, B. (2006). Reliability of MRI-derived measurements of human cerebral cortical thickness: The effects of field strength, scanner upgrade and manufacturer. *NeuroImage*, 32(1), 180–194. <https://doi.org/10.1016/j.neuroimage.2006.02.051>
- Jeannerod, M. (1994). The representing Brain : Neural correlates of motor imagery and intention. *Behavioral & Brain Sciences*, 17, 187–245.
- Jeannerod, M. (1995). Mental imagery in the motor context. *Neuropsychologia*, 33(11), 1419–1432. [https://doi.org/10.1016/0028-3932\(95\)00073-C](https://doi.org/10.1016/0028-3932(95)00073-C)
- Jeurissen, B., Leemans, A., Tournier, J. D., Jones, D. K., & Sijbers, J. (2013). Investigating the prevalence of complex fiber configurations in white matter tissue with diffusion magnetic resonance imaging. *Human Brain Mapping*, 34(11), 2747–2766.  
<https://doi.org/10.1002/hbm.22099>

- Karmali, F., & Shelhamer, M. (2008). The dynamics of parabolic flight: Flight characteristics and passenger percepts. *Acta Astronautica*, *63*(5–6), 594–602.  
<https://doi.org/10.1016/j.actaastro.2008.04.009>
- Kelly, C., & Castellanos, F. X. (2014). Strengthening connections: Functional connectivity and brain plasticity. *Neuropsychology Review*, *24*(1), 63–76.  
<https://doi.org/10.1007/s11065-014-9252-y>
- Koppelmans, V., Bloomberg, J. J., Mulavara, A. P., & Seidler, R. D. (2016). Brain structural plasticity with spaceflight. *Npj Microgravity*, *2*(1), 2. <https://doi.org/10.1038/s41526-016-0001-9>
- Kraeutner, S. N., Keeler, L. T., & Boe, S. G. (2016). Motor imagery-based skill acquisition disrupted following rTMS of the inferior parietal lobule. *Experimental Brain Research*, *234*(2), 397–407. <https://doi.org/10.1007/s00221-015-4472-9>
- Lebon, F., Horn, U., Domin, M., & Lotze, M. (2018). Motor imagery training: Kinesthetic imagery strategy and inferior parietal fMRI activation. *Human Brain Mapping*, *39*(4), 1805–1813. <https://doi.org/10.1002/hbm.23956>
- Lopez, C., & Blanke, O. (2011). The thalamocortical vestibular system in animals and humans. *Brain Research Reviews*, *67*(1–2), 119–146.  
<https://doi.org/10.1016/j.brainresrev.2010.12.002>
- Maguire, E. A., Gadian, D. G., Johnsrude, I. S., Good, C. D., Ashburner, J., Frackowiak, R. S. J., & Frith, C. D. (2000). Navigation-related structural change in the hippocampi of taxi drivers. *Proceedings of the National Academy of Sciences*, *97*(8), 4398–4403.  
<https://doi.org/10.1073/pnas.070039597>
- Martuzzi, R., Ramani, R., Qiu, M., Shen, X., Papademetris, X., & Constable, R. T. (2011). A whole-brain voxel based measure of intrinsic connectivity contrast reveals local changes in tissue connectivity with anesthetic without a priori assumptions on thresholds or regions of interest. *NeuroImage*, *58*(4), 1044–1050.  
<https://doi.org/10.1016/j.neuroimage.2011.06.075>
- Muller, A. M., & Meyer, M. (2014). Language in the brain at rest: new insights from resting state data and graph theoretical analysis. *Frontiers in Human Neuroscience*, *8*(April), 1–16. <https://doi.org/10.3389/fnhum.2014.00228>
- Naito, Y. (2003). Cortical correlates of vestibulo-ocular reflex modulation: a PET study. *Brain*, *126*(7), 1562–1578. <https://doi.org/10.1093/brain/awg165>
- Oldfield, R. C. (1971). The assessment and analysis of handedness: The Edinburgh inventory. *Neuropsychologia*, *9*(1), 97–113. [https://doi.org/10.1016/0028-3932\(71\)90067-4](https://doi.org/10.1016/0028-3932(71)90067-4)

- Ombergen, A. Van, Laureys, S., Sunaert, S., Tomilovskaya, E., Parizel, P. M., & Wuyts, F. L. (2016). Space flight-induced neuroplasticity in humans as measured by MRI : what do we know so far ? *Npj Microgravity*, (November), 0–1. <https://doi.org/10.1038/s41526-016-0010-8>
- Pearson-Fuhrhop, K. M., & Cramer, S. C. (2010). Genetic Influences on Neural Plasticity. *Pm&R*, 2(12), S227–S240. <https://doi.org/10.1016/j.pmrj.2010.09.011>
- Picard, N., & Strick, P. L. (1996). Motor areas of the median wall: a review of their location and functional activation. *Cerebral Cortex*, 6(July), 342–353. <https://doi.org/10.1093/cercor/6.3.342>
- Picard, N., & Strick, P. L. (2001). Imaging the premotor areas. *Current Opinion in Neurobiology*, 11(6), 663–672. [https://doi.org/10.1016/S0959-4388\(01\)00266-5](https://doi.org/10.1016/S0959-4388(01)00266-5)
- Raffelt, D. A., Tournier, J. D., Smith, R. E., Vaughan, D. N., Jackson, G., Ridgway, G. R., & Connelly, A. (2017). Investigating white matter fibre density and morphology using fixel-based analysis. *NeuroImage*, 144, 58–73. <https://doi.org/10.1016/j.neuroimage.2016.09.029>
- Raz, N., Lindenberger, U., Rodrigue, K. M., Kennedy, K. M., Head, D., Williamson, A., ... Acker, J. D. (2005). Regional brain changes in aging healthy adults: General trends, individual differences and modifiers. *Cerebral Cortex*, 15(11), 1676–1689. <https://doi.org/10.1093/cercor/bhi044>
- Roberts, D. R., Albrecht, M. H., Collins, H. R., Asemani, D., Chatterjee, A. R., Spampinato, M. V., ... Antonucci, M. U. (2017). Effects of Spaceflight on Astronaut Brain Structure as Indicated on MRI. *New England Journal of Medicine*, 377(18), 1746–1753. <https://doi.org/10.1056/NEJMoa1705129>
- Roberts, R. E., Anderson, E. J., & Husain, M. (2010). Expert cognitive control and individual differences associated with frontal and parietal white matter microstructure. *Journal of Neuroscience*, 30(50), 17063–17067. <https://doi.org/10.1523/JNEUROSCI.4879-10.2010.Expert>
- Rodd, J. M., Davis, M. H., & Johnsrude, I. S. (2005). The neural mechanisms of speech comprehension: fMRI studies of semantic ambiguity. *Cerebral Cortex*, 15(8), 1261–1269. <https://doi.org/10.1093/cercor/bhi009>
- Ruby, P., & Decety, J. (2004). How would You feel versus how do you think She would feel? A neuroimaging study of perspective-taking with social emotions. *Journal of Cognitive Neuroscience*, 16(6), 988–999. <https://doi.org/10.1162/0898929041502661>
- Scholz, J., Klein, M. C., Behrens, T. E. J., & Johansen-Berg, H. (2009). Training induces

- changes in white-matter architecture. *Nature Neuroscience*, *12*(11), 1370–1371.  
<https://doi.org/10.1038/nn.2412>
- Schulz, L., Ischebeck, A., Wriessnegger, S. C., Steyrl, D., & Müller-Putz, G. R. (2018). Action affordances and visuo-spatial complexity in motor imagery: An fMRI study. *Brain and Cognition*, *124*(May), 37–46. <https://doi.org/10.1016/j.bandc.2018.03.012>
- Sladky, R., Stepniczka, I., Boland, E., Tik, M., Lamm, C., Hoffmann, A., ... Windischberger, C. (2016). Neurobiological differences in mental rotation and instrument interpretation in airline pilots. *Scientific Reports*, *6*(June), 1–6. <https://doi.org/10.1038/srep28104>
- Smith, S. M., Jenkinson, M., Johansen-Berg, H., Rueckert, D., Nichols, T. E., Mackay, C. E., ... Behrens, T. E. J. (2006). Tract based spatial statistics: voxelwise analysis of multi-subjects diffusion data. *NeuroImage*, *31*(4), 1487–1505.  
<https://doi.org/10.1016/j.neuroimage.2006.02.024>
- Smith, S. M., Jenkinson, M., Woolrich, M. W., Beckmann, C. F., Behrens, T. E. J., Johansen-Berg, H., ... Matthews, P. M. (2004). Advances in functional and structural MR image analysis and implementation as FSL. *NeuroImage*, *23*(SUPPL. 1), 208–219.  
<https://doi.org/10.1016/j.neuroimage.2004.07.051>
- Smith, S. M., & Nichols, T. E. (2009). Threshold-free cluster enhancement: Addressing problems of smoothing, threshold dependence and localisation in cluster inference. *NeuroImage*, *44*(1), 83–98. <https://doi.org/10.1016/j.neuroimage.2008.03.061>
- Solodkin, A., Hlustik, P., Chen, E. E., & Small, S. L. (2004). Fine modulation in network activation during motor execution and motor imagery. *Cerebral Cortex*, *14*(11), 1246–1255. <https://doi.org/10.1093/cercor/bhh086>
- Song, S. K., Yoshino, J., Le, T. Q., Lin, S. J., Sun, S. W., Cross, A. H., & Armstrong, R. C. (2005). Demyelination increases radial diffusivity in corpus callosum of mouse brain. *NeuroImage*, *26*(1), 132–140. <https://doi.org/10.1016/j.neuroimage.2005.01.028>
- Tesink, C. M. J. Y., Petersson, K. M., Berkum, J. J. A. Van, Buitelaar, J. K., & Hagoort, P. (2014). Unification of Speaker and Meaning in Language Comprehension : An fMRI Study. *Journal of Cognitive Neuroscience*, *21*(11), 2085–2099.
- Tribukait, A., & Eiken, O. (2005). Semicircular canal contribution to the perception of roll tilt during gondola centrifugation. *Aviation Space and Environmental Medicine*, *76*(10), 940–946.
- Tribukait, A., & Eiken, O. (2006). Semicircular canal influence on the visually perceived eye level during gondola centrifugation. *Aviation Space and Environmental Medicine*, *77*(5), 500–508.

- Tribukait, A., & Eiken, O. (2012). Flight experience and the perception of pitch angular displacements in a gondola centrifuge. *Aviation Space and Environmental Medicine*, 83(5), 496–503. <https://doi.org/10.3357/ASEM.3038.2012>
- Tribukait, A., Grönkvist, M., & Eiken, O. (2011). The perception of roll tilt in pilots during a simulated coordinated turn in a gondola centrifuge. *Aviation Space and Environmental Medicine*, 82(5), 523–530. <https://doi.org/10.3357/ASEM.2898.2011>
- Van Ombergen, A. (2017). *The effect of microgravity and vestibular disorder on human neurplasticity*. Antwerp University.
- Van Ombergen, A., Heine, L., Jillings, S., Roberts, R. E., Jeurissen, B., Van Rompaey, V., ... Wuyts, F. L. (2017). Altered functional brain connectivity in patients with visually induced dizziness. *NeuroImage: Clinical*, 14, 538–545. <https://doi.org/10.1016/j.nicl.2017.02.020>
- Van Ombergen, A., Wuyts, F. L., Jeurissen, B., Sijbers, J., Vanhevel, F., Jillings, S., ... Demertzi, A. (2017). Intrinsic functional connectivity reduces after first-time exposure to short-term gravitational alterations induced by parabolic flight. *Scientific Reports*, 7(1), 1–10. <https://doi.org/10.1038/s41598-017-03170-5>
- Zempleni, M. Z., Renken, R., Hoeks, J. C. J., Hoogduin, J. M., & Stowe, L. A. (2007). Semantic ambiguity processing in sentence context: Evidence from event-related fMRI. *NeuroImage*, 34(3), 1270–1279. <https://doi.org/10.1016/j.neuroimage.2006.09.048>
- Zhang, S., & Li, C. shan R. (2012). Functional connectivity mapping of the human precuneus by resting state fMRI. *NeuroImage*, 59(4), 3548–3562. <https://doi.org/10.1016/j.neuroimage.2011.11.023>
- Zu Eulenburg, P., Caspers, S., Roski, C., & Eickhoff, S. B. (2012). Meta-analytical definition and functional connectivity of the human vestibular cortex. *NeuroImage*, 60(1), 162–169. <https://doi.org/10.1016/j.neuroimage.2011.12.032>